45kW Full Bridge Converter with Discontinuous Primary Current for High Efficiency Airborne Application

Y. Bouvier, M Vasic, P. Alou, J. A. Oliver, O. García, J. A. Cobos

***Abstract*—This paper presents and describes the design and optimization process of a high power density 45kW DC/DC converter for aircraft application. This converter is a part of an isolated rectifier for a military aircraft pulsating load. It has to provide galvanic isolation and good stability when the load steps as high as 40 kW are applied. In order to obtain high efficiency, on the primary side of the converter a discontinuous triangular current modulation is implemented. High power density is obtained by relatively high switching frequency of 10 kHz and by implementation of the transformer using a nanocrystalline material that enables high magnetic flux density (up to 1T) and copper foils for conductors. The expected efficiency of the converter is 97.6% and the total weight of the system is 7.6 kg.**

I. Introduction

There is a strong tendency in aircraft designs towards a More Electric aircraft (MEA). This concept is the consequence of the substitution of pneumatic, mechanic and hydraulic equipments by electrical equipment. This increase in electric loads inside the aircrafts causes the need for bigger and more efficient power supply solutions.

To cope with this increase of electrical power, in the area of military aircraft, the traditional voltage levels of $28V_{DC}$ has evolved to $270V_{DC}$. One of the main benefits of this high voltage is that the current levels are 10 times lower than with conventional low voltage. Therefore, it is possible to reduce the section of wires and by that reduce also the weight, which is a key variable in aircraft design. One of the most complicated loads that have to be supplied from $270V_{DC}$ bus is the high power pulsating load, where the load steps can be as high as 40kW. Additionally, this type of the load requires galvanic isolation, high power factor, low current THD and good control of the supply voltage. Table I shows short overview of the electrical specifications for the aforementioned pulsating load.

A possible solution for this application is a three stage active rectifier. The first stage is an input EMI filter to attenuate the harmonics of the system, followed by a two stage power converter with an intermediate DC bus. An active rectifier AC/DC converter provides a constant DC bus to an isolated DC/DC converter. Figure 1 show simplified block diagram of the system.

TABLE I
SPECIFICATIONS FOR THE AC-DC CONVERTER

Input voltage	V_{IN}	115V AC
Output voltage	V_{OUT}	270V DC
Output power	P_{OUT}	45 kW
Temperature range	T	-55º to +85º
Target weight	W	45 kg

This paper is going to focus on the design and optimization of the DC/DC converter.

A. DC/DC Converter Specifications

This DC/DC converter has to be designed for an aircraft application. The primary concern for the design is to have a high power density, in other words, to have good efficiency as well as low weight. The output voltage is 270V and the power range is from 0W to 45kW. The possibility to parallelize the converter is required as well, because the load is a 90 kW pulsating load.

This converter is for a military application, so it has to meet the functional requirements as well as the standards for environmental and operational conditions. A military derating of 25% is applicable to temperatures in thermal designs as well as the breakdown voltage of the devices.

The input voltage of this converter is the output of the rectifier stage and it is not determined and has to be optimized. The DC bus value influences the selection of devices. The higher the input voltages to the DC/DC converter, the lower are the currents that have to be processed and this have high impact to conduction losses. However, the high voltage is usually correlated with high switching losses of the active devices. Additionally, if we assume that the primary side is implemented as a full bridge converter, for an input voltage of 450V, applying the military derating, we need to choose devices of 600V breakdown voltage. If the input voltage is higher than 450V, the 1200V devices must be selected. These two types of devices have different switching characteristics and voltage drop during the conduction and it can be easily seen how the selection of the intermediate bus voltage and military derating have a direct influence on the overall efficiency.

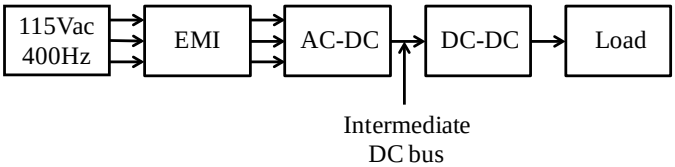

Fig. 1. Simplified block diagram of the system

B. Comparison of isolated DC/DC converter topologies

Four isolated DC/DC converter topologies are analyzed for this application: Full bridge phase shifted dual active bridge,

resonant dual active bridge and triangular full bridge.

All the chosen topologies are of full-bridge type in order to take advantage of a full excursion of the magnetic field in the transformer and to take full advantage of the magnetic core.

1) Full bridge Phase Shifted converter

The full-bridge phase-shift is a robust converter that has high power density and efficiency [2]. However, the transistors on the primary side always are turned on with high switching losses. The diodes on the secondary side are turned off by applying negative voltage between its terminals and in order to avoid power losses due to reverse recovery, Schottkey diodes should be used. Having in mind the high voltage that the secondary diodes have to withstand, the only solution for them is the SiC diodes that have high conduction losses and penalizes the overall efficiency.

2) Dual active Bridge

This topology uses two sets of full bridges to achieve a bidirectional converter. This converter can also have a triangular modulation of the current and can have only one magnetic component if the leakage is used as the inductor. The bidirectional behavior is not needed in our design and it is needed to have 8 controllable switches which is additional complexity in the design.

3) Dual Active Bridge Series Resonant Converter

The Bidirectional Dual Active Bridge Series Resonant Converter (DAB SRC) [3] is a type of dual active bridge that attenuates switching losses by the use of a resonant capacitor in series with the leakage inductance of the transformer. The main advantage of this topology is the ZVS in all switches at cost of a more complicated control. Also the output voltage cannot be controlled it is always proportional to the input voltage. Another advantage of this topology is the bidirectional power transfer, but in the case of our application it is not useful.

4) Triangular Current Waveform Full-Bridge

The Triangular current waveform full-bridge is a topology that uses the leakage inductance of the transformer to achieve a triangular current waveform and has ZCS in the primary switches [6]. It also minimizes the reverse recovery effect in the secondary bridge.

The main advantages of the triangular full-bridge are the soft transitions in the diode bridge and in the primary switches, and that it only needs one magnetic component, given that the leakage inductance can be used as the inductor of the converter. Due to the fact that the leakage inductance of the transform is used to shape the primary current, and that this current has high ripple, high capacitance is needed at the output. This capacitance can occupy significant volume and it is a drawback of this topology.

II. Proposed Topology

The chosen topology for the DC/DC converter is the triangular full bridge for the reasons explained before. The schematic of the converter's circuit can be seen on Fig. 2. The circuit is composed of only one magnetic component, the transformer, a bridge of transistors in the primary and a bridge of diodes in the secondary. A capacitor is also needed in the output to filter and absorb the load steps.

A. Principle of Operation

Figure 3 shows the current of the transformer secondary and its voltage. First Powering state, from t_0 to t_1, S1 and S4 switches are turned ON. The input voltage is applied to the primary of the transformer and the output voltage to the secondary. The current rises linearly due to the leakage inductance of the transformer. In secondary side, diodes D5 and D9 are conducting the output current. The slope of the current can be calculated with the following equation.

$$\frac{\Delta I_t}{\Delta t} = \frac{(n \cdot V_{IN} - V_{OUT})}{L_\sigma} \quad (1)$$

First freewheeling state, from t_1 to t_2, S1 is turned OFF and after a dead-time S2 is turned ON. The current flows through the parallel diode D2 and S4. The voltage applied to the primary is zero and the output voltage in the secondary side, so the current drops linearly and the slope is calculated with this equation.

$$\frac{\Delta I_t}{\Delta t} = \frac{-V_{OUT}}{L_\sigma} \quad (2)$$

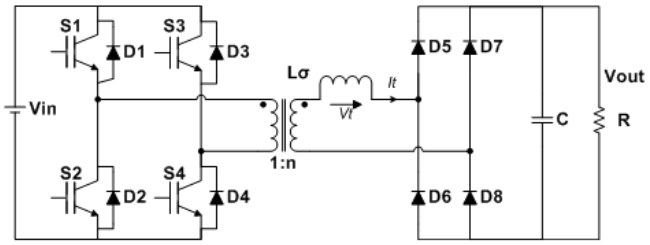

Fig. 2. Schematic of the triangular current full-bridge.

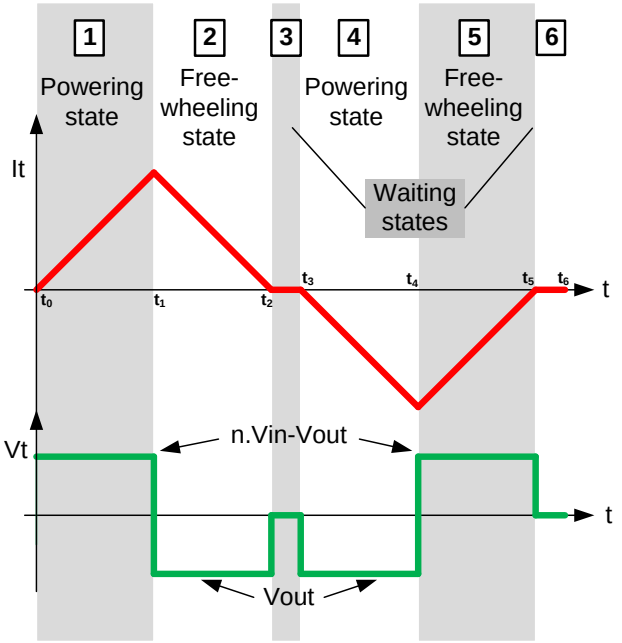

Fig. 3. Transformer current and voltage waveforms and switching stages of a full period.

First waiting state, from t_2 to t_3, the current has finally reached zero. A small sinusoidal current due to the resonance of the leakage inductance and diode parasitic capacitance can be observed during this time interval.

Second powering state, from t_3 to t_4, S3 and S2 are turned ON. The current decreases to negative values. This stage is

equivalent to the t_0 to t_1 stage. In the secondary side, D6 and D7 are conducting the output current.

Second freewheeling state, from t_4 to t_5, S3 is turned OFF and S2 is turned ON, the current flows through D4 and S2.

Second waiting state, from t_5 to t_6, the current in the transformer is zero and the next switching cycle can begin.

The principal advantage of this topology is the soft switching of the devices. There are only two hard switching in both high-side transistors in a switching cycle, at t_1 for S1 and at t_3 for S3. Also the diodes in the secondary side are always turn ON and OFF softly, reducing the problem of reverse recovery in those devices.

To achieve ZCS in the primary transistors it is fundamental to avoid continuous conduction. This can be done with an accurate control of the slopes in the triangular current. The equations (1) and (2) define the slopes for the triangle waveform. The input voltage V_{IN}, the turn's ratio n and the leakage inductance L_σ are critical parameters in the design of this topology.

In order to avoid continuous conduction mode the parameters have to comply with the following equation:

$$\frac{n \cdot V_{IN}}{V_{OUT}} \frac{L_\sigma \cdot \Delta I_t}{(n \cdot V_{IN} - V_{OUT})} \leq \frac{T_s}{2} \quad (3)$$

If the triangle shape is symmetrical, then, we have an additional equation fixing the value for t

$$n = \frac{2 \cdot V_{OUT}}{V_{IN}} \quad (4)$$

In one half of the switching cycle the current has to rise and fall in time. A good design solution, to take into account transient and load steps is to give some amount of wait time (t_3 to t_4 and t_5 to t_6) in order to have a safe margin and never reach the continuous conduction mode.

The high side switches are the ones having hard switching so they have more losses than the low-side devices. Freewheeling states are always taken with the low side switches ON to achieve better balance of power losses.

B. Component selection

The frequency range for this application is between 10 kHz to 30 kHz. In that range and considering the high power nature of this converter, IGBT's are a good choice for the primary transistor. The use of MOSFET was analyzed at frequencies up to 30 kHz and no significant advantages in power losses or weight were found.

With MOSFET's there is the need to parallelize three devices per switch, which is not the case for IGBT. Finally, IGBT modules can be found with integrated driver [1]. This simplifies and adds to the robustness of the design.

The weight of the transformer is reduced by increasing the frequency and for the magnetic material nanocrystalline from VITROPERM has been selected due to the fact that high magnetic flux densities can be reached (up to 1T).

C. Transformer Design

As seen in the previous section, the transformer is a fundamental element in this topology. The leakage inductance and the turn's ratio are both critical variables in the design.

For this application, where the weight is critical, there is the need for low core losses and high saturation voltage to reduce the transformer core size and also reduce the amount of turns and therefore reduce the overall weight of the transformer.

VITROPERM 500 [8] is a new core material made of nanocrystalline. This material has a very flat hysteresis cycle and has therefore less core losses than conventional ferrites. Usually nanocrystalline material can give transformer design with as much as half of size and weight as conventional ferrites.

The current through the transformer is triangular and the converter needs to operate in discontinuous conduction mode. This triangular shape is high in harmonic content, so even if the switching frequency is low (10 kHz), we have to consider the high frequency nature of the harmonics to design the windings of the transformer.

Two options are possible to cope with the high frequency problem in the windings, Litz wires or the use of copper or aluminum foil, to limit the skin effect and make use of most of the conductors sections. The high voltage of the application dismisses the use of Litz wires. To eliminate completely the skin effect the foil needs to have a thickness double than the skin depth. We choose to eliminate the first, third and fifth harmonic so the skin depth is around 0.3 mm and the foil must be 0.6 mm thick.

The use of foils for the windings limits the possibility to interleave the windings to have a good coupling, but the topology needs a fair amount of leakage to be able to work. On the other hand, a specific value of leakage inductance is required by the converter to operate so this value needs to be accurately estimated.

The estimation of the leakage inductance of a transformer by analytical method is difficult because of the nature of the problem. The leakage inductance is a parasitic and there is no exact equation to accurately estimate its value. The use of finite element program was required. The final design of the transformer is summarize in table II

TABLE II
FINAL DESIGN OF TRANSFORMER

Core	T60102-L2-157-W159 VITROPERM
Primary turns	14
Secondary turns	10
Fill Factor	0.25%
Leakage inductance	4μH to 8μH (tests need)
Core losses (iGSE)	17W
Copper losses	89W
Total losses	106W
Total weight	4.1 kg

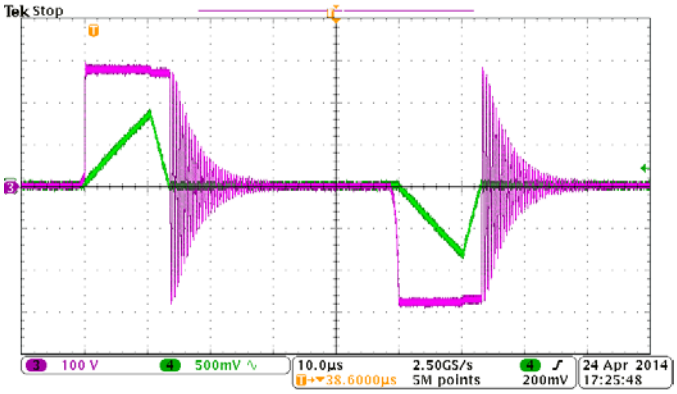

Fig. 4 Current of the secondary of the transformer (green) and secondary voltage of the transformer (pink).

D. Power Losses Calculations

In order to estimate the efficiency of this converter, an accurate calculation of losses in the devices as well as in the transformer is needed.

The core losses are calculated following the approach in [4] and [5].The magnetizing current in the transformer is of trapezoidal nature. The Steinmetz equation is only completely valid for sinusoidal waveform. To accurately calculate the core losses of the transformer we use the improved Generalized Steinmetz Equation (iGSE).

$$P_V = \frac{1}{T}\int_0^T k_i \left|\frac{dB}{dt}\right|^{\alpha} (\Delta B)^{\beta-\alpha}\, dt \tag{5}$$

Where ΔB is peak to peak flux and,

$$k_i = \frac{k}{(2\pi)^{\alpha-1}\int_0^{2\pi}\left|\cos\theta\right|^{\alpha}\cdot 2^{\beta-\alpha}\, d\theta} \tag{6}$$

The parameters k, α and β are the same parameters as used in the Steinmetz Equation (6). By use of the iGSE losses of any flux waveform can be calculated, without requiring extra characterization of material parameters beyond those for the Steinmetz Equation.

Another factor in the optimization and calculation of losses for the transformer is the rounding effect in the number of turns. Turns are discrete so the real turns ratio can differ from the ideal one. In the case of our design it limits the maximum ΔB. Figure 4 shows calculated copper and core losses for the selected transformer core (T60102-L2-157-W159 VITROPERM).

The reverse recovery of the diodes in the secondary side bridge can be neglected because the topology is forcing them to turn on and off with zero current. However, if the negative current slope is high this loss mechanism cannot be neglected and it is needed to calculate those losses if the asymmetry in the triangle is very high.

Calculation of losses in IGBT is done by using the following equation.

$$P_{losses} = V_{CE}\cdot I_{AVG} + R_{CE}\cdot I_{RMS}^2 \tag{7}$$

Values for V_{CE} and R_{CE} are taking with the maximum temperature in order to have a conservative design.

The losses in the parallel diode with the IGBT are also required because they are conducting during the wait times, since IGBT are unidirectional switches.

Once the power losses are calculated, thermal analysis is required to know what type of cooling system to choose. To maximize the power density, liquid cooling is required for the primary transistors, the transformer and the secondary diode bridge. This also minimizes the converters volume and weight because conventional heat sinks will be too big to fit the target weight and size.

E. Optimization

The conduction losses are determined by the topology and by the output power specification. In the other hand, switching losses can be lowered, with a correct modulation of the triangle current

There is only two non-zero current switching in one switching cycle and the amount of energy that is lost in those transitions depends on the peak of the triangular current and the value of the DC bus voltage. In order to reduce this amount of energy loss and therefore reduce the switching losses the modulation and the turn's ratio of the transformer can be changed to have an asymmetrical triangle.

From equation (3) we can derive the following equation:

$$\Delta I_t = \frac{K\cdot T_s}{2}\cdot\frac{V_{OUT}}{n\cdot V_{IN}}\cdot\frac{(n\cdot V_{IN}-V_{OUT})}{L_\sigma} \tag{8}$$

Where K is a constant defining the ratio of time that the current is not zero over half period.

We can analyze the effect of changing the turns ratio n by calculating the partial derivative of (8):

$$\frac{d(\Delta I_t)}{dn} = \frac{K\cdot T_s}{2}\cdot\frac{V_{OUT}}{n^2\cdot V_{IN}}\cdot\frac{V_{OUT}}{L_\sigma} \geq 0 \tag{9}$$

The derivative is a positive number since all of the variables included have positive value. To reduce the value of the peak of the current in the transformer it is needed to reduce the turn's ratio n. But then we have to comply with (3) to be in DCM. To achieve this, the value of the leakage inductance must be lowered. The overall effect of these changes is that the rising of the current is slower than the fall, and so the triangle has so the same base but lower height, so lower value of the peak current. With this method the switching losses can be lowered, because the peak current of the hard switching is lower.

In the other hand, the turns ratio must be lower, and depending on the transformer design the copper losses can be increased as well. The asymmetrical shape of the current is responsible for more losses by reverse recovery in the diodes, because the slope of the fall is steeper than in the symmetrical triangle. Figure 5 shows simulated current and voltage at the secondary winding of the transformer.

There is a trade of between losses that needs to be analyzed for particular cases to have the most efficient solution.

TABLE III
POWER LOSSES BREAKDOWN

Component	Weight	Power Losses
IGBT- APTGT400A60D3G	1.2 kg	600 W
Diodes – MEE 300-06DA	0.6 kg	340 W
Transformer	4.3 kg	130 W
Capacitors EPCOS B32778 10 x 110 µF = 1100 µF	0.5 kg	8 W
Total	**6.6k**	**1078W**

The DC bus voltage is not restricted by specification, so it's a variable to be taken in to account for optimizing the overall efficiency of the converter. The higher the voltage in the DC bus, the higher the breakdown voltage of the primary transistor is. But with a high voltage in the bus, the currents are lower thus reducing the switching losses in primary. Although, the optimization of the DC voltage can also affect the AC-DC design, in this particular design, lowering the DC voltage bus was more beneficial to the AC-DC than detrimental to the DC-DC converter, so a voltage of 450V has been selected. Based on this analysis, the selected IGBT modules are APTGT400A60D3G while the rectifier diodes are MEE 300-06DA. Table 3 shows the breakdown of power losses and the weight of each part of the converter is shown as well.

F. Design of control loop

This converter is controlled with peak current mode. This mode is chosen because of the need to parallelize the converter. Another benefit of this control method is that by measuring the input peak current, a short circuit and overcurrent protection can be easily implemented.

Two loops are required for this control, the peak current loop as well as the voltage loop to control the output voltage. As the current in the leakage inductor is fixed by the topology, it stops being a state variable.

The equivalent averaged circuit to control consists of two dependant current sources, modeling the primary and secondary currents of the transformer. The primary averaged transformer current can be calculated with the following equation.

$$I_{AVG1} = \frac{n \cdot V_{IN}}{V_{OUT}} \cdot \frac{L_\sigma \cdot \Delta I_t^2}{(n \cdot V_{IN} - V_{OUT}) \cdot T_s} \qquad (10)$$

The secondary averaged current, which is the output current, can be derive from (equation) easily with the power balance in the transformer.

The transfer function of the system depends on the output voltage, input voltage and current in the transformer (equation). This transfer function is highly non-linear. In order to simulate, an approximate linearized model is made and simulations are run with the software SIMPLIS. The result of the transfer function in open loop can be seen in Fig. 6. A full range of power loads is analyzed in order to design a regulator able to deal with the pulsating load.

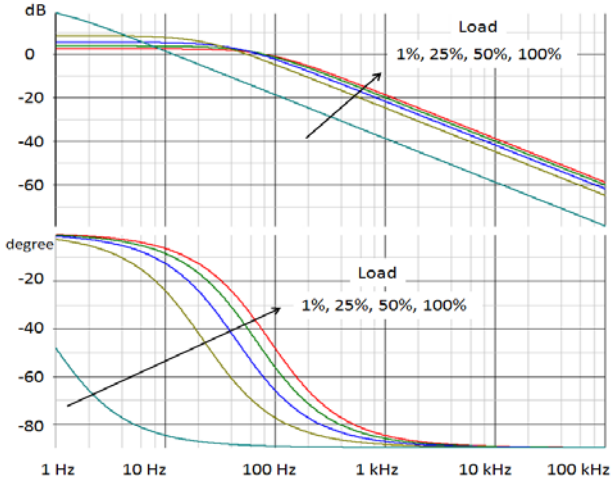

Fig. 5. Open loop Vout/Ipeak transfer function for different power loads.

The loop is closed at around one decade below the switching frequency to have as much bandwidth as possible. The phase margin is verified for multiple loads in simulation. A compensator with a 62 Hz zero and a 6.2 kHz pole has been designed. We put two decades between the zero and the pole to give a boost of phase in a wide range, and reach reasonable phase margin for all the loads. The ideal value to reach for phase margin is 72º. We can see in Fig. 7 that for all the load steps the phase margin is between the 70º to 80º lines.

A summary of the phase margin per load condition can be seen in table IV.

The system is required to be stable for a given pattern of power load steps shown in figure 8. The military standard defines that the output voltage has to be inside a given limits during the transition time after the load steps, Figure 9.

Simulations are run to verify the stability and dynamics of the converter defined in Fig. 7. The simulation verifies the dynamic requirements that can be seen in Fig. 8.The output voltage rise is less than 6V and the recovery of the steady state is done in less than 30ms.

TABLE IV
PHASE MARGIN WITH DIFFERENT LOADS

	1% Load	25% Load	50% Load	75% Load	100% Load
Phase margin	**71º**	**79º**	**77º**	**76º**	**75º**

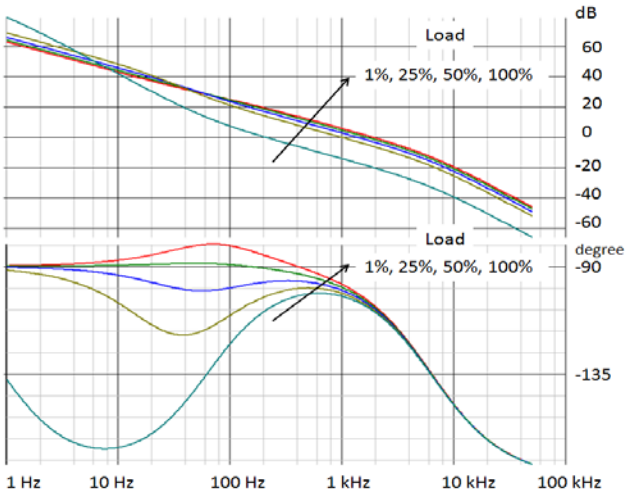

Fig. 6. Close loop gain transfer function for different power loads.

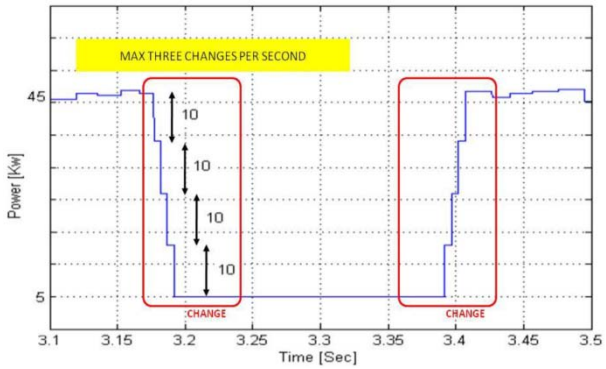

Fig. 7. Power steps of the aircraft pulsating load.

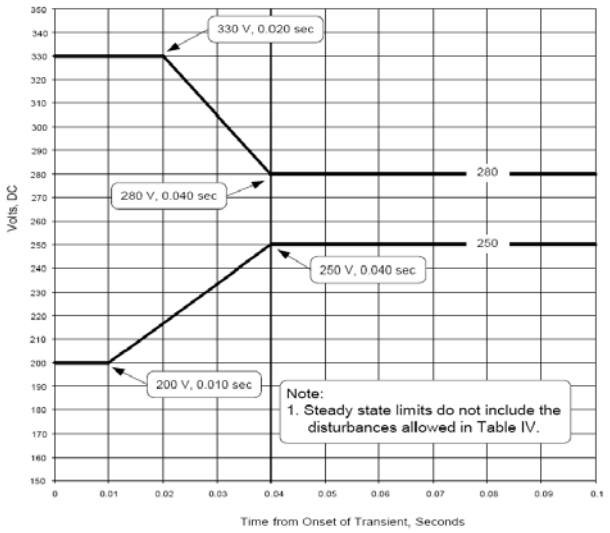

Fig. 8. Dynamic limits for the output voltage after load steps.

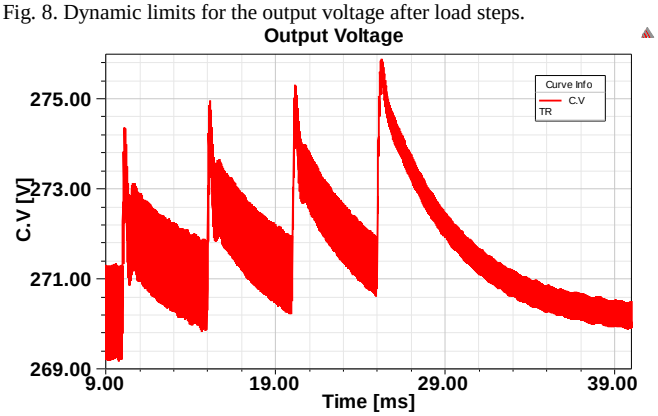

Fig. 9. Simulation result the output voltage after the four load steps.

III. Final Design and Construction.

A summary of the characteristics and specifications of the final design can be seen in table V.

The mechanical construction of the prototype has been under process and in the final version of the paper complete experimental results will be shown. Figure 11 shows how the prototype will look like. It can be noticed that copper rails have been used to make connections where the high frequency current is running (between the diode bridge and output capacitor) in order to minimize conduction losses.

TABLE V
Final Design of DC-DC Prototype

Input voltage	450V DC
Output voltage	270V DC
Leakage inductance	4μH to 8μH (tests needed)
Output capacitor	1.1 mF
Output voltage ripple	2.1V (0.77%)
Output power	45 kW
Total power losses	1078 W
Efficiency	97.6%
Total weight	7.6 kg

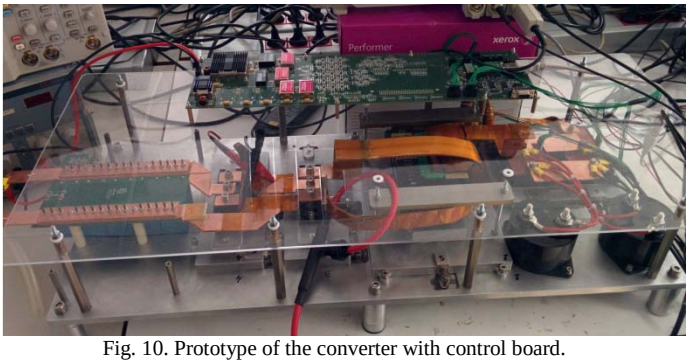

Fig. 10. Prototype of the converter with control board.

IV. Conclusions

A design process for a 45kW DC/DC converter based on a full bridge converter with discontinuous current in the primary has been presented. This converter is used as a final stage of a three stage active rectifier with isolation that has to supply high power pulsating load. This topology shows advantages comparing it with other solutions due to its simplicity and high efficiency that comes from the fact that almost all the devices are turned on/off with zero current. Additionally, this topology does not need any additional output or input inductor and therefore the overall weight can be reduced as well. After the optimization process it has been shown that the shape of the current has to asymmetric in order to obtain low power losses. High power density and high power efficiency of the converter are obtained thanks to the liquid cooling system that will be applied. The converter that has been designed is expected to have efficiency around 97.6% and weight around 7.6kg and it will be able to supply correct output voltage under the load steps as high as 40kW.

References

[1] Mircosemi IGBT modules, APTLGT400A608G. Onlinehttp://www.microsemi.com/existing-parts/parts/85224

[2] J. Biela, D. Christen, J. W. Kolar "Optimization of a 5-kW Telecom Phase-shift DC-DC converter With Magnetically Integrated urrent Doubler"

[3] Z. Pavlović; J. A. Oliver; P. Alou; Ó. Garcia; J. A. Cobos "Bidirectional Dual Active Bridge Series Resonant Converter with Pulse Modulation"

[4] J.Li, T. Abdallah, and C. R. Sullivan, "Improved calculation of core loss with nonsinusoidal waveforms."

[5] K. Venkatachalam, C. R. Sullivan, T. Abdallah, and H. Tacca, "Accurate prediction of ferrite core loss with nonsinusoidal waveforms using only Steinmetz parameters."

[6] I. D. Jitaru "A 3kW Soft Switching DC-DC Converter" http://www.rompower.com/Papers/A%203kW%20Soft%20Switching%20DC-DC%20Converter.pdf

[7] Bernardo Cougo and Johann W. Kolar, ETH Zurich "Integration of Leakage Inductance in Tape Wound Core Transformers for Dual Active Bridge Converters"

[8] "Nanocrystalline cut cores made of VITROPERM® 500 for transformers" Online: http://www.vacuumschmelze.com/fileadmin/Medienbiliothek_2010/Produkte/Kerne_und_Bauelemente/Anwendungen/Kerne/Schnittbandkerne/Cut_Cores_flyer_2011.pdf